Enzyme catalysis: Transition structures and quantum dynamical aspects: Modeling rubisco's oxygenation and carboxylation mechanisms

ARTICLE *in* INTERNATIONAL JOURNAL OF QUANTUM CHEMISTRY · JANUARY 2002

Impact Factor: 1.43 · DOI: 10.1002/qua.10116

5 AUTHORS, INCLUDING:

Orlando Tapia
Uppsala University
236 PUBLICATIONS **4,265** CITATIONS
SEE PROFILE

Vicent S Safont
Universitat Jaume I
84 PUBLICATIONS **1,423** CITATIONS
SEE PROFILE

Enzyme Catalysis: Transition Structures and Quantum Dynamical Aspects: Modeling Rubisco's Oxygenation and Carboxylation Mechanisms

O. TAPIA,[1] HENK FIDDER,[1] VICENT S. SAFONT,[2] MÓNICA OLIVA,[2] JUAN ANDRÉS[2]

[1]*Department of Physical Chemistry, Uppsala University, Box 532, S-75121 Uppsala, Sweden*
[2]*Departament de Ciències Experimentals, Universitat Jaume I, Box 224, 12080 Castelló, Spain*

Received 13 September 2001; accepted 16 October 2001
DOI 10.1002/qua.10116

ABSTRACT: Quantum dynamics is introduced with the help of molecular states (MS) for systems decomposable into n electrons and N nuclei. These states, when projected onto the electronic and nuclear configuration spaces, **r** and **R**, respectively, are represented as products of electronic and nuclear wave functions of the type $\Phi_{\mathbf{k}}(\mathbf{r};\alpha_k^\circ)\chi_{\mathbf{kj}}(\mathbf{R};\alpha_k^\circ)$. The $3N$ coordinates α_k° are the positions of positive charges in real space that are equivalent to the nuclear charges. The stationary geometry is derived from quantum chemical analytical gradient optimization procedures. The set $\{\Phi_{\mathbf{k}}(\mathbf{r};\alpha_k^\circ)\chi_{\mathbf{kj}}(\mathbf{R};\alpha_k^\circ)\}$ is assumed to contain all cluster partitioning including corresponding asymptotic states. These MSs provide a basis to represent a quantum state as a particular linear superposition. Quantum states are (row) vectors in a dual space whose components are the complex coefficients in the linear superposition of MSs. A reactive system is represented in the direct product space of the MS and surrounding medium: $|\mathrm{MS}\rangle \otimes |\mathrm{E}\rangle$. The surrounding basis states $\{|E\rangle\}$ may be other molecular state systems (protein, solvent) or electromagnetic fields. A chemical reaction is represented as a time evolution of vectors in the dual space driven by the interaction with an energy source or sink system. A theory of catalysis is constructed on this new basis for which the protein–substrate interaction operator drives the quantum change of state. The chemical reaction catalyzed by rubisco is examined and used to introduce the theoretical scheme. The mechanism of carboxylation and oxygenation expressed as sets of transition structures is discussed from this new quantum mechanical perspective. For a protein in thermal equilibrium with a thermal bath at absolute temperature T, in so far as time evolution in the reactant system is concerned, the protein may be replaced by a blackbody radiation field. In real situations, both the protein–substrate and electromagnetic field–substrate interactions provide mechanisms to favor particular time evolutions of the quantum system. A mapping to a unit hypersphere with the axis

Correspondence to: O. Tapia; e-mail: orlando.tapia@fki.au.se.

represented by (orthogonalized) MSs permits a simple "visualization" of all bound quantum states related to the system as points on the surface of the hypersphere. Time evolution of complex systems can be systematized in this new way. Int J Quantum Chem 88: 154–166, 2002

Key words: quantum dynamics; *n* electrons; *N* nuclei; sink system; carboxylation and oxygenation

Introduction

Recently, carboxylation [1] and oxygenation chemical reactions [2] catalyzed by the enzyme rubisco, have been theoretically characterized with the help of hydroxypropanone, C^1H_3—C^2O—C^3H_2OH, modeling the chemically active groups in the substrate D-ribulose-1,5-bisphosphate (RuBP). The transition structures (T-Ss) were obtained to describe enolization, and carbon dioxide and oxygen fixation, followed by hydration and C^2—C^3 bond breaking. Specific to oxygenation is the concerted breaking of O—O and C—C bonds, while carboxylation involves a configuration inversion at the C^2 center after the carbon–carbon snipping step.

Enzyme-activated RuBP reacts with carbon dioxide, leading to atmospheric carbon dioxide fixation at its C^2 center. The mechanism involves a complex chemical reaction starting from the enolization step and followed by the sequence summarized in Figure 1. Two molecules of 3-phospho-D-glycerate (PGA) are released from the active site. An equally complex situation is found for the oxygenation mechanism. In Figure 2 we introduce the set of transition structures and intermediates describing the oxygenation chemical reaction obtained from ab initio analytical gradient methods.

In a number of reports we have shown that all the carboxylation and the oxygenation chemical reactions can be described with a minimal 3-carbon (3C) molecular model [3, 4] and have tested a 5-carbon (5C) molecular model giving identical results [5]. In the enzymatic carboxylation chemistry studied by us, for each step, a well-defined T-S describes the conversion with the help of related precursor and successor complexes. The successor complex of a given step appears as a partner to form the precursor complex of the following step. These findings lead to the intramolecular mechanistic description of Figure 1. At variance with early mechanistic proposals that were based upon general acid/base catalysis by selected residues of the enzyme [6–8], the picture developed by us is fully self-contained in a molecular model sustaining all the chemical reactions. This gives us the opportunity to apply recent theories in which quantum mechanics is fully implemented after the Born–Oppenheimer (BO) scheme is cured from its classical physics approach of electronic and nuclear state separation [9–13].

The studies of T-Ss in vacuum have given rise to skepticism. It is a common belief that the enzyme

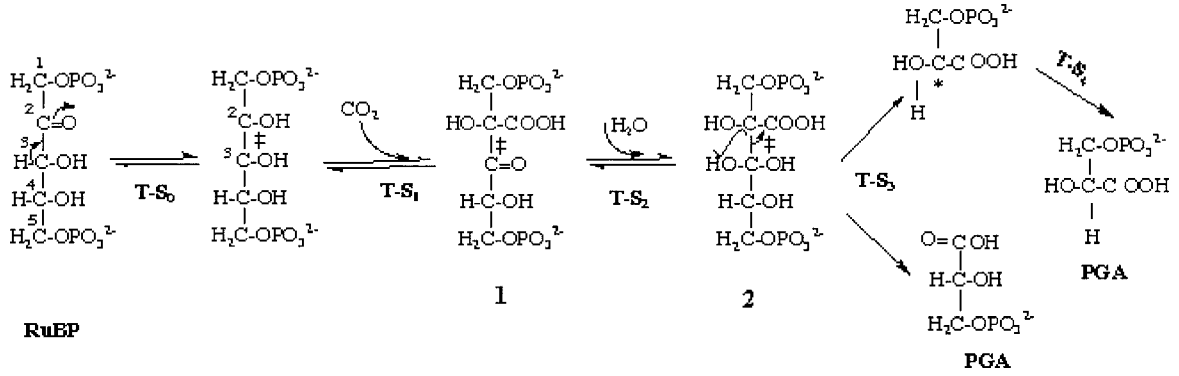

FIGURE 1. Mechanism for the carboxylation of RuBP catalyzed by rubisco. The reactants, products, and putative intermediates are shown. The substrate is first enolized (through $\mathbf{TS_0}$). Carbon dioxide is fixated at the C^2 center of the enediol (via $\mathbf{TS_1}$). Hydration of the resulting carbonyl group at C^3 ($\mathbf{TS_2}$) leads to the intermediate **2**. C^2—C^3 bond cleavage with concomitant H migration yields one product (PGA) molecule ($\mathbf{TS_3}$). A final step with configuration inversion at C^2 and H transfer to C^2 (via $\mathbf{TS_4}$) gives the second PGA molecule.

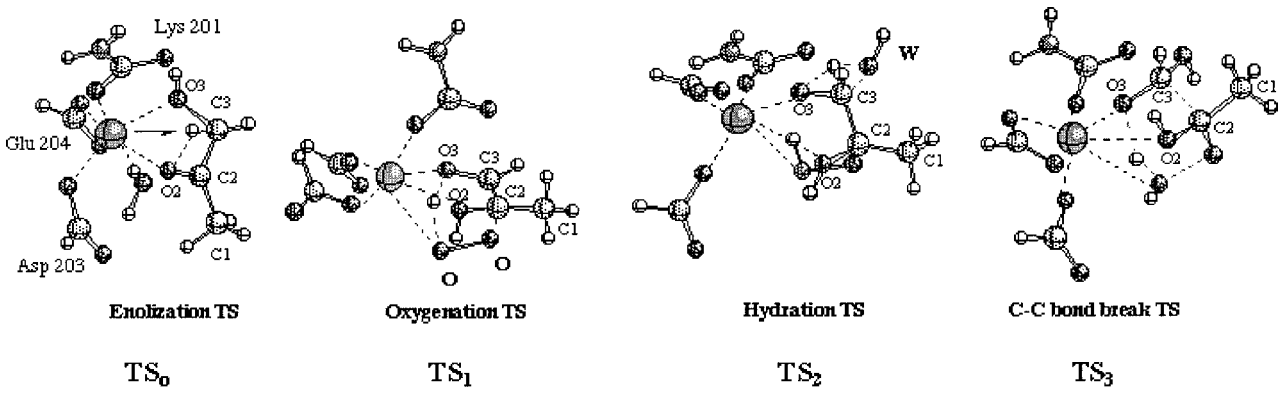

FIGURE 2. Mechanism for the oxygenation of RuBP catalyzed by rubisco. The transition structures associated with the different steps are shown. The molecular model used in the calculations represents the real RuBP substrate with hydroxypropanone (CH_3COCH_2OH) and includes a representation of the magnesium coordination sphere. This consists of two formate anions representing Asp 203 and Glu 204 and a carbamate representing the carbamylated Lys 201. Starting from the coordinated substrate the set of steps results in the formation of product molecules PGA and phosphoglycolate in the real system and a water molecule. Note that this molecule can stay coordinated to Mg, thus recovering the original coordination sphere.

will somehow change the structure of the transition structures obtained in vacuum. The theoretical problem has been to evaluate the role played by the enzyme. The question was: Is there any reason to believe that, once the complexities of the active site are introduced in the calculations, one would get the same mechanistic picture in terms of similar transition structures? The answer has general implications for molecular modeling. As discussed below, there are many more aspects to the role of the protein that can be discussed from the standpoint of our models in the absence of the enzyme. However, for the present system the more serious criticism came from the fact that magnesium is essential for catalysis. Moreover, to activate the protein, a lysine residue should react with a carbon dioxide molecule (different from the one entering in the carboxylation step), leading to a carbamate. This modified residue together with an aspartate and a glutamate provides the coordination shell for magnesium. What is the effect of magnesium on the saddle point structures characterizing the T-Ss of the minimal molecular model? To take care of these criticisms, the model substrate was embedded in the Mg coordination shell including a model carbamylated lysine.

The results were most rewarding [1, 2]. Figure 2 illustrates the concatenated sequence of transition structures found in the Mg-coordination shell for oxygenation. The geometry invariance was proved for all but one case, namely, enolization ($\mathbf{TS_0}$). The comparison of $\mathbf{TS_0}$ with the corresponding T-S without the Mg shell offered a beautiful example of the catalytic effect at the electronic level. But this was not all. The geometrical invariance of the carbon framework to interactions and the fact that this framework can be superposed onto the crystal structure of the 2-carboxy-D-arabinitol 1,5-bisphosphate (CABP) inhibitor complex determined by Andersson [14] are also important results. They prompted the exploration of the possibility of using a full quantum mechanical treatment of the enzyme–substrate system. We investigate in this article this possibility and give a framework in which the principles of state-to-state chemical reactions in a complex system can at least be easily formulated. A complete quantum mechanical description will be introduced below starting from well-known facts found in our experience of calculating the geometry of stationary structures [15].

Stationary Structures

The stationary structures, obtained with the powerful analytic first and second derivatives techniques, do not involve the nuclear masses. The energy E is a function of the geometry of external sources of Coulomb potential representing only the charges on the nuclei, $E(\alpha)$, with α representing the position of the external charges. In practical calculations, an auxiliary Hamiltonian is used (although we never acknowledge this to be so): $H_e(\mathbf{r}, \alpha)$, where $\mathbf{r}$ is the position vector operator for the n electrons, $\mathbf{r} = (\mathbf{r}_1 \cdots \mathbf{r}_n)$, while $\alpha = (\alpha_1 \cdots \alpha_N)$

stands for the coordinates *in real space* of sources whose electric charges match those of the nuclei. The difference may seem subtle; the consequences are, however, most decisive as we will see in a moment [9]. In Cartesian coordinates, the Hessian is used as a potential energy to solve the nuclear Schrödinger equation. Diagonalizing it yields six zero eigenvalues (five for linear molecules) where three eigenvectors correspond to the free translation of the inertial frame implicitly used and the other three give the direction cosines for a frame related to the stationary geometry. We assume all stationary species to be determined in the same laboratory frame. The $3N-6$ remaining degrees of freedom define the so-called normal modes. For the saddle point of index 1, a further degree of freedom is subtracted to the vibration normal modes ($3N-7$). This is well known. What is less known is the fact that the electronic wave function rendering stationary the functional $E(\alpha)$ at a value, say α_k°, $\Phi_{\mathbf{k}}(\mathbf{r};\alpha_k^\circ)$, can be used to construct a basis beyond the BO framework [9]. The set of $\{\Phi_{\mathbf{k}}(\mathbf{r};\alpha_k^\circ)\}$ for the same attractor at α_k° forms a set of orthogonal electronic wave functions as they are solutions to the same Hamiltonian $H_e(\mathbf{r},\,\alpha)$. Those belonging to different attractors are linearly independent and can be, if required, orthogonalized. In this orthogonal subspace, it can be easily shown that the total molecular Hamiltonian, $H(\mathbf{r},\mathbf{R}) = K_N + H_e(\mathbf{r},\mathbf{R})$, becomes diagonal [9, 11–13, 16]:

$$\begin{aligned} E_k(\mathbf{R}) &= \left\langle \Phi_{\mathbf{k}'}(\mathbf{r};\alpha_{k'}^\circ)\middle| H(\mathbf{r},\mathbf{R})\Phi_{\mathbf{k}}(\mathbf{r};\alpha_k^\circ)\right\rangle \\ &= E(\mathbf{R},\alpha_k^\circ)\delta_{kk'}. \end{aligned}$$

Each electronic wave function defines an attractor for the set of N external positive charges. This is the fundamental property assigned to this type of function. The total wave function is now formed as a product with the nuclear $\chi_{\mathbf{kj}}(\mathbf{R};\alpha_k^\circ)$ and the associated electronic wave function $\Phi_{\mathbf{k}}(\mathbf{r};\alpha_k^\circ)$. The product $\Psi_{\mathbf{kj}} = \Phi_{\mathbf{k}}(\mathbf{r};\alpha_k^\circ)\chi_{\mathbf{kj}}(\mathbf{R};\alpha_k^\circ)$ is a solution to the total time-independent Schrödinger equation $H\Psi = E\Psi$ once we solve the nuclear Schrödinger equation,

$$\begin{aligned} \left(K_N + \left\langle \Phi_{\mathbf{k}}(\mathbf{r};\alpha_k^\circ)\middle| H_e(\mathbf{r},\mathbf{R})\middle|\Phi_{\mathbf{k}}(\mathbf{r};\alpha_k^\circ)\right\rangle\right)\chi_{\mathbf{kj}}(\mathbf{R};\alpha_k^\circ) \\ = E_{kj}\chi_{\mathbf{kj}}(\mathbf{R};\alpha_k^\circ). \quad (1) \end{aligned}$$

Note that $\langle\Phi_{\mathbf{k}}(\mathbf{r};\alpha_k^\circ)|H_e(\mathbf{r},\mathbf{R})|\Phi_{\mathbf{k}}(\mathbf{r};\alpha_k^\circ)\rangle = E_k(\mathbf{R};\alpha_k^\circ)$, which is precisely what we calculate in actual computing of a stationary geometry. The difference is that now we cannot move the sources of charges as we could do with the auxiliary electronic Hamiltonian $H_e(\mathbf{r},\alpha)$.

The configuration space $\mathbf{R}$ is the space where the nuclear quantum basis states are projected; it is not indicating the position of the nuclei. Now, a wave function is defined everywhere in the $\mathbf{R}$ space. The energy expectation value, $E_{k'}(\mathbf{R};\alpha_k^\circ)$ in Eq. (1), acts as a potential energy function. There are no constraints upon the $\mathbf{R}$ domain at variance with the BO scheme. This theory treats electron and nuclei quantum states on a similar basis, i.e., there are no constraints set upon the corresponding configuration spaces. The geometry α_k° permits introduction of noncompact (point) groups to label the electronic wave function. This is a rigorous result. Let us now examine the solutions to the global electronic–nuclear problem and the representation of chemical processes.

For a given Hamiltonian representing a set of n electrons and N nuclei, the molecular basis states are formed from all clusters conserving the total charge. The column vector $[\Psi_{\mathbf{00}}, \Psi_{\mathbf{01}}, \Psi_{\mathbf{02}}, \ldots, \Psi_{\mathbf{k0}}, \Psi_{\mathbf{k1}}, \Psi_{\mathbf{k2}}, \ldots, \Psi_{\mathbf{k'0}}, \Psi_{\mathbf{k'1}}, \ldots]$ stands for the molecular basis ordered by the increasing energy expectation value. A row vector such as $(0,0,\ldots,0,0,\ldots,1,0,\ldots)$ can be interpreted as if the system were in the k' electronic state and the ground vibration state, symbolized by, say, $\Psi_{\mathbf{k'0}}$. Any row vector but $(1,0,0,\ldots 0,\ldots)$ requires a history of interactions (preparation) with external energy sources. It is imperative to realize that the quantum label k is not restricted to a single chemical species. It labels all electronic states that at sufficiently high energy can be put in resonance with $n+N$ free-particle states. A row vector may characterize a chemical species as an asymptotic state. A chemical reaction involves changes of amplitudes along different electronic states. In the old language, a molecule characterized by $\Phi_{\mathbf{k}}(\mathbf{r};\alpha_k^\circ)$ undergoes a chemical reaction if it "moves" to a new quantum state $\Phi_{\mathbf{k}'}(\mathbf{r};\alpha_{k'}^\circ)$. In the present view, the basis set is fixed and always there; only the amplitudes change in the row vector. The set of basis functions is orthogonal and with $H(\mathbf{r},\mathbf{R})$ being diagonal in the basis of molecular stationary states, an external interaction field is required to mediate a physical chemical process, i.e., a change in quantum state. We will use the coupling to an external electromagnetic field to mediate transitions: $V = -\mathbf{A}\cdot\mathbf{p}$, where $\mathbf{A}$ is the transverse electromagnetic potential and $\mathbf{p}$ is the total linear momentum operator for the composite of "$n+N$ particles," $\mathbf{p} = \mathbf{p}_n + \mathbf{p}_N$. To first order in the coupling operator, the product gives the vector transition amplitude

$$\begin{aligned} \mathbf{T}_{k'j'}^{kj} = \left\langle \Phi_{\mathbf{k}}(\mathbf{r};\alpha_k^\circ)\middle|\mathbf{p}_n\middle|\Phi_{\mathbf{k}'}(\mathbf{r};\alpha_{k'}^\circ)\right\rangle \\ \times \left\langle \chi_{\mathbf{kj}}(\mathbf{R};\alpha_k^\circ)\middle|\chi_{\mathbf{k'j'}}(\mathbf{R};\alpha_{k'}^\circ)\right\rangle_R. \quad (2) \end{aligned}$$

The overlap integral $\chi_{\mathbf{kj}}(\mathbf{R};\alpha_k^\circ)|\chi_{\mathbf{k'j'}}(\mathbf{R};\alpha_{k'}^\circ)\rangle_R$ is the well-known Franck–Condon factor from electronic spectroscopy. For now, the change from reactants to products is represented as an electronic transition. This is a characteristic result from the present theory.

For a standard chemical reaction where each reactant is in a closed shell ground electronic state, the electronic parity is +1 in both the reactant and product channels. The first-order reaction rate is zero because the operator **p** has parity −1. A finite rate will emerge from first-order, second-order, and higher-order processes involving parity −1 intermediate quantum states. The state of lowest energy having adequate parity is what we call a quantum transition state (QTS).

The possibility found in the theory to define inertial frames is also a new result [11–13, 16]. In principle, the general quantum theory is formulated as a set of equations, Dirac and Maxwell equations, whose form is essentially determined by relativistic invariance. Atomic basis states are obtained by solving the relevant differential equations [17]. In chemistry we take the nonrelativistic limits, keeping the labels related to the nonhomogeneous Lorentz group for the atomic basis (particle states, atomic orbitals). Molecular systems are treated as usual in direct product spaces conveniently symmetrized. The quantum states must be invariant to translation and rotation of the frame. This, in turn, implies linear momentum and total angular momentum conservation. This is a property bestowed on frame invariance; it applies to any molecular system. Norm invariance to time displacement leads to a time-dependent Schrödinger equation [18].

For bimolecular reactions, by definition, the reactants R1 and R2 are asymptotic states of the global system Hamiltonian. These R1 and R2 have electronic states defining local attractors (local frames) that permit defining local linear **k** vector and angular momentum quantum numbers, J and M_J. A typical quantum basis state will be characterized by the ket $|R1, \mathbf{k}_{R1}, J_{R1}, M_{J(R1)}\rangle$ that can be written now as the direct product $|R1, K_{R1}, M_{K(R1)}\rangle|\mathbf{k}_{R1}, R_{R1}, M_{R(R1)}\rangle$; the total angular momentum is separated into a frame-related and an internal angular momentum, with $J_{R1} = K_{R1} + R_{R1}$. The basis quantum states for the products, say P1 and P2, are analogously defined, e.g., $|P1, K_{P1}, M_{K(P1)}\rangle|\mathbf{k}_{P1}, R_{P1}, M_{R(P1)}\rangle$. Note that the chemical change is to be described within one and the same Cartesian frame. As illustrated by the T-Ss in Figure 2, the quantum states associated with the transition structure are obtained from a supermolecule and are included in the basis $[\Psi_{\mathbf{01}}, \Psi_{\mathbf{02}}, \ldots, \Psi_{\mathbf{k1}}, \Psi_{\mathbf{k2}}, \ldots, \Psi_{\mathbf{k'0}}, \Psi_{\mathbf{k'1}}, \ldots]$. Again, we use the frame defined by one of them to calculate the geometry of all stationary species. Coming back to the α space, distances between local frames and the supermolecule frame play the role of intermolecular distances. All apparatus used to set up and measure a chemical reaction is defined in the real α space. It is therefore apparent that a fully consistent definition of molecular shape can only be obtained from the eigensolutions to the auxiliary Schrödinger equation:

$$H_e(\mathbf{r}, \alpha_k^\circ)\Phi_{\mathbf{k}}(\mathbf{r};\alpha_k^\circ) = \varepsilon(\alpha_k^\circ)\Phi_{\mathbf{k}}(\mathbf{r};\alpha_k^\circ). \qquad (3)$$

This equation must be solved for all k's related to species with stationary geometry.

In an inertial frame there is no coupling between electronic and nuclear quantum states. A coupling can be produced if the system is "accelerated," or in other words is interacting with an external source. We will not dwell on this important issue here. The transition amplitude connecting the states ki and $k'i'$ is given by the Franck–Condon integral. Energy conservation is enforced; namely, the external energy must match the energy gap $\Delta E_{k'i'}^{ki} = E_{k'i'} - E_{ki}$ to get a finite value of $\mathbf{T}_{k'i'}^{ki}$.

The Overlap Factor

A close analysis of the transition structures depicted in Figure 2 for oxygenation shows that their shapes are complementary to the active site shape. This favors large values for the overlap integrals appearing in the relevant $\mathbf{T}_{k'i'}^{ki}$ factors because the substrates are trapped in the same **R** region. On the contrary, in solution, the probability of having the reactants in the same neighborhood of the **R** space covered by the vibration wave functions of the T-Ss appears to be almost negligible. In fact, this reaction in solution has not been detected yet, indicating that the rate is extremely small. The binding of RuBP at the active site of rubisco increases the odds of the chemical reaction. This result applies to any bimolecular reaction mediated by a supermolecule transition structure.

The Electronic Factor

The first step in the chemical mechanism is the enolization of RuBP. In a standard enolization, two

bonds are snipped and two bonds are knitted. The molecules have closed shell electronic structures; therefore, $\mathbf{T}_{\text{enol}}^{\text{keto}}$ is zero. The problem is not solved if one uses a base (B:) to collect the proton at C^3 and an acid A–H to protonate O^2. Both species (B:) and A–H are closed shell systems. In our quantum chemical language, what is needed is an activation of both C^2 and C^3 so that carboxylation or oxygenation can take place at C^2, as well as hydration at C^3. In Figure 1, the symbol ‡ was inserted between C^2 and C^3. This was done to remind the reader of the fact that the dihedral angle O^2–C^2–C^3–O^3 in CABP comes out with 60° in *cis* form. The transition structure for intramolecular enolization in the Mg coordination shell has about the same value for this angle. The most remarkable fact is that the same T-S without magnesium is almost planar. The enolization transition structure (**TS₀**, see Figs. 1 and 2) is activated by the carbamylated lysine residue. Although this is a beautiful example of catalytic activation at the theoretical level, it does not fully explain yet the parity problem because this T-S has a closed shell structure at the Hartree–Fock level of theory.

From basic quantum chemistry we know that the spin triplet has a stationary structure for a diene conformer twisted at 90°. The same is true for the dienol as we have reported in early studies [19, 20]. Now, for the sake of discussion, let us take a local frame, the z axis directed from C^3 to C^2 with origin midway, the x axis on the plane of the *cis*-conformer, and the y axis perpendicular to that plane. At 90°, the dienol will have a p_y orbital in one carbon and a p_x orbital in the other. The point is that the conversion process is related to changes in the orbital angular momentum as well as to changes in the spin angular momentum. Furthermore, at 90° the orbitals p_x and p_y are degenerate so that a diradical spin singlet state can be constructed so that the wave function of the transition structure may have a component having -1 parity either along the x or the y directions. Therefore, a QTS should have a correctly correlated electronic wave function with appropriate parity components. The transition moments $\mathbf{T}_{\text{QTS}}^{\text{keto}}$ and $\mathbf{T}_{\text{enol}}^{\text{QTS}}$ may now have positive components, thereby granting a nonzero rate.

The quantum mechanical treatment of nuclear states supersedes the classical mechanics view of nuclei as heavy particles. There is no longer a need for BO potential energy hypersurfaces which now are reduced to useful computing tools in the search for stationary geometry states. Even though one may "picture" vibrational states as classical nuclear motion (normal modes), for quantum dynamics only the set of electronuclear quantum states is relevant. In other words, the concept of vertical excitations is not granted because the overlap integral is between vibration wave functions and not nuclear positions. The linear superpositions of nuclear wave functions are formed instantaneously upon interaction with the electromagnetic field. The calculation of rates and representation of mechanisms, in general, can be carried out with the help of time-dependent quantum theory. What are then the objects of time evolution? The molecular basis set is fixed. The quantum states of the system are linear superpositions. Time evolution can accomplish changes in the nature of the linear superposition, which can be interpreted as possible chemical reactions.

Chemical Reactions as a Quantum Dynamical Problem

The substrate and enzyme systems are represented by their Hamiltonians, H_S and H_E, respectively. The total Hamiltonian H includes the Coulomb interaction operator, H_{SE}. If we designate the basis state functions as $|\mathrm{S}, k, i\rangle$ and $|\mathrm{E}, j, g\rangle$ for the substrate and enzyme in the absence of interaction (asymptotic systems), the global system basis states will be represented as the set of direct products: $|\mathrm{S}, k, i\rangle \otimes |\mathrm{E}, j, g\rangle$. Entangled states between both systems are neglected for the time being. A quantum state of the asymptotic systems, $|\mathrm{S}\rangle$ and $|\mathrm{E}\rangle$, is given by the linear superposition,

$$|\mathrm{S}\rangle = \sum_{ik} \langle \mathrm{S}, k, i|S\rangle |\mathrm{S}, k, i\rangle = \sum_{ik} s_{ki} |\mathrm{S}, k, i\rangle \qquad (4)$$

and

$$|\mathrm{E}\rangle = \sum_{jg} \langle \mathrm{E}, j, g|E\rangle |\mathrm{E}, j, g\rangle = \sum_{jg} e_{jg} |\mathrm{E}, j, g\rangle. \qquad (5)$$

The k, i quantum numbers represent electronic and nuclear quantum states of the substrate system; j, g identify the electronic and nuclear states of the enzyme (we have added labels S, E for identification purposes). A quantum state of the global system $|\Phi\rangle$ in this model is a simple product of substrate and enzyme states: $|\Phi\rangle = |\mathrm{S}\rangle|\mathrm{E}\rangle$. It is important to note that the basis states are obtained as solutions of all auxiliary electronic Schrödinger Eqs. (3) in combination with Eq. (1). A similar procedure is undertaken for the enzyme, although in practice simple models are constructed.

Let us prepare a particular quantum state of the global system at time, say $t = t_0$, and study

the state of the system at a later time t: $|\Phi, t\rangle = U(t, t_0)|\Phi, t_0\rangle$, where $U(t, t_0)$ is the standard unitary time evolution operator [18]. In our case, it is given by $U(t, t_0) = \exp(-iH(t-t_0)/\hbar)$ with the total Hamiltonian $H = H_0 + H_{SE}$. H_0 is the asymptotic operator $H_S + H_E$:

$$|\Phi, t\rangle = U(t, t_0)|S\rangle|E\rangle = \exp\big(-iH(t-t_0)/\hbar\big) \times \sum_{ik}\sum_{jg} e_{jg}s_{ki}|S, k, i\rangle|E, j, g\rangle. \quad (6)$$

The formal solution to Eq. (6) is a series in interaction representation:

$$\begin{aligned}|\Phi, t\rangle &= U(t, t_0)|S, t_0\rangle|E, t_0\rangle \\ &= \left[\hat{1} + (-i)\int_{t_0}^{t} dt_1\, H_I(t_1) \right. \\ &\quad \left. + (-i^2)\int_{t_0}^{t} dt_1 \int_{t_0}^{t_1} dt_2\, H_I(t_1)H_I(t_2) + \cdots\right] \\ &\quad \times |S, t_0\rangle|E, t_0\rangle. \end{aligned} \quad (7)$$

The interaction operator is defined by $H_I(t) = \exp(iH_0(t-t_0))H_{SE}\exp(-iH_0(t-t_0))$.

For a time period $(t - t_0)$ sufficiently long so that we can consider the subsystems noninteracting again, the solution to Eq. (7) will have a set of new coefficients. The time evolution leads to a new set $\{e'_{jg}s'_{ki}\}$ and, since the basis states are associated with stationary states of all possible molecular species, the chemical process is to be read from the changes of the coefficients in the dual space: $\{e_{jg}s_{ki}\}$ goes to $\{e'_{jg}s'_{ki}\}$.

The basis states for bound systems are normalized, so that any linear superposition can be mapped onto a vector of a unit radius hypersphere. Any point on the surface of this hypersphere maps a particular linear superposition. Time evolution can be pictured as "trajectory swaths" on this hypersurface. A particular swath depends, among other things, on the energy contained in the system.

Let us consider a simple model to see how this theory works when chemical pictures are used. The keto–enol transformation is pertinent since it is present in the enolization step (cf. Figs. 1 and 2). The molecular basis set contains quantum states for the keto, enol, and quantum transition state: $|\text{keto}\rangle$, $|\text{enol}\rangle$, and $|\text{QTS}_0\rangle$. The keto and enol quantum states are linearly independent. Even if they are not orthogonal, a simple transformation would solve that problem: $|+\rangle = 1/\sqrt{2}\,(|\text{keto}\rangle + |\text{enol}\rangle)$ and $|-\rangle = 1/\sqrt{2}\,(|\text{keto}\rangle - |\text{enol}\rangle)$. We note the power of the new theory: there is no adiabatic nuclear transformation (minimal energy path in the BO scheme) transforming the eigenstates of Eq. (3). The initial state $|\text{keto}, t_0\rangle$ is the keto form, $(1/\sqrt{2}, 1/\sqrt{2}, 0)$:

$$|\text{keto}\rangle = 1/\sqrt{2}\,|+\rangle + 1/\sqrt{2}\,|-\rangle + 0|\text{QTS}_0\rangle. \quad (8)$$

The state which we are interested in is the enol one, $(1/\sqrt{2}, -1/\sqrt{2}, 0)$ to within a phase factor:

$$|\text{enol}\rangle = \exp(i\pi)\big(1/\sqrt{2}\,|+\rangle - 1/\sqrt{2}\,|-\rangle + 0|\text{QTS}_0\rangle\big). \quad (9)$$

The transition amplitude to obtain enol states starting from the keto is given by the overlap between the time evolved initial state, $U(t, t_0)|\text{keto}\rangle$:

$$\begin{aligned}&\langle\text{enol}|\text{keto}, t\rangle \\ &\quad = \big\langle\text{enol}\big|U(t, t_0)\big|\text{keto}, t_0\big\rangle \\ &\quad = \left\langle\text{enol}\right|\Big(-i^2\Big)\int_{t_0}^{t} dt_1 \int_{t_0}^{t_1} dt_2\, H_I(t_1)H_I(t_2) + \cdots \\ &\qquad + \left|\text{keto}, t_0\right\rangle \\ &\quad = \left\langle\text{enol}\right|\Big(-i^2\Big)\int_{t_0}^{t} dt_1 \int_{t_0}^{t_1} dt_2\, H_I(t_1)\Big|\text{QTS}_0\Big\rangle \\ &\qquad \times \big\langle\text{QTS}_0\big|H_I(t_2)\big|\text{keto}, t_0\big\rangle + \cdots. \end{aligned} \quad (10)$$

In the second line of Eq. (10), the two other components of the identity resolution do not contribute to the transition integral due to parity selection rules.

There is a second type of process permitting the change of quantum state from the keto to the transition state. The process is first order because $\langle\text{QTS}_0|(-i)\int_{t_0}^{t_1} dt_1\, H_I(t_1)|\text{keto}, t_0\rangle = \mathbf{T}_{TS}^{keto}$ has parity $+1$. And from $|\text{QTS}_0\rangle = (0, 0, 1)$ the system may evolve to the enol state, $(1/\sqrt{2}, -1/\sqrt{2}, 0)$, because the parity of

$$\left\langle\text{enol}\right|(-i)\int_{t_0}^{t} dt_1\, H_I(t_1)\Big|\text{QTS}_0\Big\rangle = \mathbf{T}_{enol}^{TS} \text{ is } +1.$$

The product of the two integrals measures the amplitude with which this process occurs. This is easy to understand since at a given time t, the interaction may drive the system into a coherent superposition $|\Phi, t\rangle$ with a nonzero coefficient at the $|\text{QTS}_0\rangle$: $|\Phi\rangle = a_1|+\rangle + a_2|-\rangle + a_3|\text{QTS}_0\rangle$.

This model can be examined by using a simple mapping: $x \leftrightarrow |+\rangle$, $y \leftrightarrow |-\rangle$, and $z \leftrightarrow |\text{QTS}_0\rangle$. All linear superposition states can hence be mapped onto a sphere of unit radius where a vector with components $(\sin\theta\cos\phi, \sin\theta\sin\phi, \cos\theta)$ represents a normalized linear superposition:

$$|\theta, \phi\rangle = \sin\theta\cos\phi|+\rangle + \sin\theta\sin\phi|-\rangle + \cos\theta|\text{QTS}_0\rangle. \quad (11)$$

The reaction starts from the keto form, and the initial state at the enzyme active site has $\theta = \pi/2$ and $\phi = \pi/4 + 2n\pi$, with $n = 0, \pm 1, \ldots$; we take here $n = 0$. The $|\text{keto}\rangle$ state is represented by this coherent state. The probability of getting an amplitude for $\theta = \pi/2$ and $\phi = \pi/4 + \pi$ is zero because $\mathbf{T}^{\text{keto}}_{\text{enol}}$ has parity -1. Once the time evolution is set up, the unit vector is displaced either to the upper or lower hemisphere. This means that θ will take values smaller or larger than $\pi/2$. This situation will evolve sooner or later into ϕ larger than $\pi/4$. Any time that ϕ attains a value $\pi/4 \pm \pi$, the coherent superposition would represent the $|\text{enol}\rangle$ quantum state with 100% probability. The swaths on the unit surface connecting $(1/\sqrt{2}, 1/\sqrt{2}, 0)$ to $(1/\sqrt{2}, -1/\sqrt{2}, 0)$ are always mediated by states having a nonzero component for the transition state. It is implicit in this example that the basis states have the same energy: time evolution takes place in an energy shell. This type of coherent state can be used to include an "activated complex" with a finite lifetime. The activated complex embodies the QTS and the precursor and successor quantum states. These latter are obtained by vibration excitations of appropriate subsets in the vibration spectrum of the corresponding stationary molecular states as they are derived from solutions to the auxiliary Schrödinger Eqs. (3) and (1). It is rewarding to see that the model contains a natural mechanism for time recurrence (chemical clocks).

Catalysis: Energetic and Quantum Dynamical Aspects

The enolization step can now be qualitatively discussed in a quantum dynamics picture. To fix ideas, in Figure 3 we introduce a simple model to describe catalytic effects. The asymptotic system enzyme plus reactant ($E + R_0$) and enzyme plus product ($E + P_0$) have energies corresponding to an endothermic process. We take as an example a system having a large activation energy in vacuum. An energy E is allocated to the system, which is not enough to overcome the activation barrier in vacuum. The reactant system interacting with the protein structure is denoted as $E{:}S_i$. The symbol E: is the protein in its active form, S_i has the energy of the reactant dressed with the interaction energy. The energy level $E{-}R_i$ is a putative complex where the substrate has the same geometry as in the asymptotic form. In other words, all the protein binding energy is used to stabilize the complex level $E{-}R_i$. The substrate states interacting with the protein are assumed to have an energy lower than that in vacuum. The energy $E{:}QTS_{if}$ is the lowest electronic energy of the quantum transition state. Since the stationary geometry of QTS_{if} is basically invariant in going from vacuum to the active site of the enzyme, all binding energy is realized as a coarse T-S stabilization.

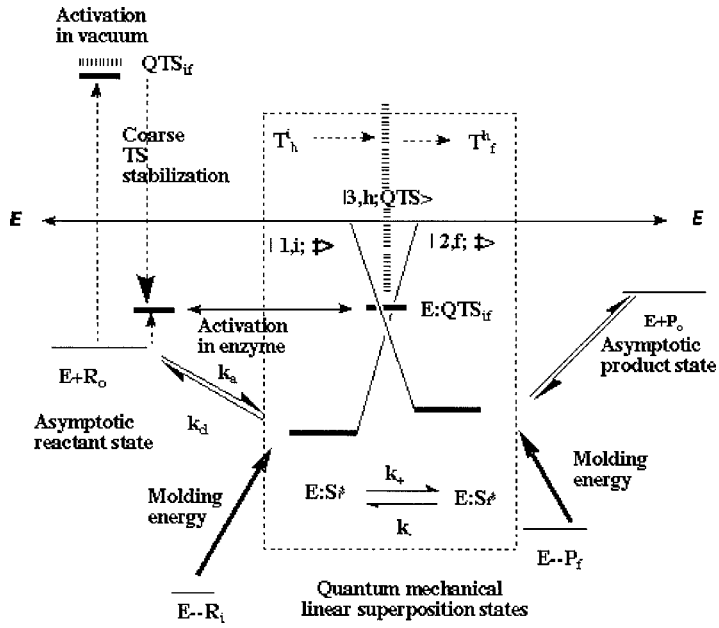

FIGURE 3. Schematic representation of the quantum dynamics picture for the enolization step (see text).

Let us examine the reaction inside the activated protein. The quantum states there have been written in a compact manner. In fact, for instance, $|1, \mathrm{i}; \ddagger\rangle$ stands for a direct product $|1, \mathrm{i}\rangle|0, \mathrm{g}; \mathrm{E}\rangle$ where the substrate vibration level is above or equal to the E:QTS lowest vibration level. We assume, that as an initial condition the enzyme has amplitude 1 along the ground electronic state base vector; g is a collective vibration quantum label. The enzyme (protein), by being a large macromolecule, has a large density of states in the region above the activation threshold.

To study the nature of the linear superposition states, let us consider the keto–enol example discussed above. Now, the assignments are $|\mathrm{keto}\rangle \rightarrow |1\rangle$, $|\mathrm{enol}\rangle \rightarrow |2\rangle$ and including the vibration numbers we define the new basis states:

$$|+; \mathrm{i}, \mathrm{f}\rangle = 1/\sqrt{2}\left(|1, \mathrm{i}; \ddagger\rangle + |2, \mathrm{f}; \ddagger\rangle\right) \qquad \text{and}$$
$$|-; \mathrm{i}, \mathrm{f}\rangle = 1/\sqrt{2}\left(|1, \mathrm{i}; \ddagger\rangle - |2, \mathrm{f}; \ddagger\rangle\right);$$
$$|\mathrm{QTS}\rangle = |3, \mathrm{h{:}QTS}\rangle.$$

As a result of binding, $\{|1, \mathrm{i}; \ddagger\rangle\}$ are specific excited vibration levels of the molded keto form, and analogously $\{|2, \mathrm{f}; \ddagger\rangle\}$ are levels for the molded enol form. These vibration states have amplitudes overlapping with the transition state vibrations. Naturally, the dimension of the hypersurface of the real system is tremendously higher than 3. Many among them will contribute to the total transition amplitude, thereby leading to a relevance of considering the density of states. Understanding the dominance of certain (exit) channels hinges on two aspects: (1) the relative density of states at these channels and (2) relaxation rates into other manifolds (intramolecular vibration relaxation and relaxation involving electromagnetic fields that are always present and effectively infinitely degenerate).

If the protein is in thermal equilibrium at absolute temperature T, in as far as energy exchanges are concerned, the protein can be modeled as a blackbody radiation system at temperature T. The operator $V = \mathbf{A} \cdot \mathbf{p}$ in the Heisenberg representation would then enter the formulae (7) and (10). This is an important result, for now we can see that a blackbody radiation field of appropriate temperature may act as a catalyst [21]. In view of the small energy gaps one may have at the QTS, a microwave blackbody may actively modulate chemical reactions [22].

In so far as catalytic effects described in a more chemical vein are concerned, one can distinguish a global uniform effect as well as differential effects. Surface complementarity, as derived from our transition structures, suggests that it will be these states which are most stabilized (cf. Fig. 3).

In Figure 3 we have emphasized a theoretical effect we have denoted as molding energy [23]. This is a quantity that can be calculated by determining the energy difference between the lower energy conformer of a substrate and the energy the substrate would have if we impose a geometry (α-space calculation) similar to the one found in the transition structure for the corresponding fragment. The molding energy is a property that depends upon the protein. Observe the close relation between this quantity and the activation energy in the scheme. If the protein–substrate interaction energy were used to stabilize the substrate then the activation energy inside the enzyme would be larger. Consequently, one of the roles of the enzyme has to be destabilization of the substrate ground state structures. Stabilization would make the substrate an active site inhibitor! In the same way, the products should also not be stabilized, since their release from the protein will be the rate-limiting step. In Figure 3, the ratio k_a/k_d corresponds to the Michaelis constant, K_m. Thus, if K_m increases, one would expect a slower reaction step.

Oxygenation Chemistry

Before examining quantum dynamical aspects, let us consider the nature of the oxygen–protein complex. Oxygen $^3O_2$, due to its spin state, does not interact strongly with any portion of the protein. To do this, another triplet state is required. Therefore, no standard Michaelis complex can be expected since the $|1, g; {}^3\mathrm{E}\rangle$ state, which signals the first triplet state of the protein itself, may be too high in energy to participate noticeably in the linear superposition states. The lowest energy oxygenation T-S is a spin singlet; the intersystem crossing must then take place with the enolization successor molecular state [2, 24]. Rubisco's experimental kinetics follows a modified Theorell–Chance mechanism; the process is sequentially ordered: RuBP binds first. After enolization, oxygen reacts with second-order kinetics without first forming a Michaelis complex [25, 26]. The agreement of the theoretical results with the kinetic mechanism is then quite satisfactory.

The basis states for the quantum dynamical description must be complemented with those of oxygen and the oxygenation TS_1. The triplet state and

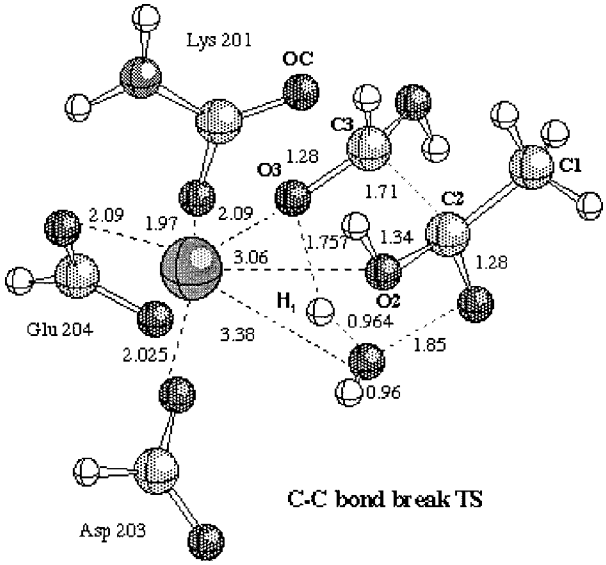

FIGURE 4. Transition structure for the C—C and O—O bond-breaking step, as obtained with the model that includes the magnesium coordination sphere.

TABLE I
Main components of the transition vector.

3C model		Mg model	
Component	Value	Component	Value
d(C3–O3)	−0.119	*d*(C3–O3)	−0.199
d(C2–C3)	0.543	*d*(C2–C3)	0.505
d(O–O′)	0.528	*d*(O–O′)	0.650
d(Ht–O′)	−0.262	*d*(Ht–O′)	−0.130
A(C2–C3–O3)	0.122	*A*(Ow–C3–O3)	−0.107
Z(H3–C3–Ow–Hw)	−0.118	*A*(H3–C3–Ow)	0.105

T-S for C—C and O—O bond breaking. Distances (*d*) in Å; angles (*A*) and dihedrals (*Z*) are in degrees. The computing methods (Hartree–Fock, 6-31G** basis set) are the same as those reported earlier [2]. All calculations were carried out using the Gaussian 94 [28] and Gaussian 98 [29] programs. Supplementary vibration analysis is made with the GaussView [30] package.

diradical states and any other electronic state related to the supermolecules that are obtained from Eq. (3) are part of the molecular basis set. The link between enolization and oxygenation does not involve keto states.

Intersystem crossing (triplet–singlet) must take place at this point in the mechanistic scheme. For, as TS_1 suggests, the chemical reaction will proceed now on the spin singlet manifold. The time evolution on the spin singlet hypersurface will reflect the chemical mechanism in a relatively simple manner. The successor quantum states interacting with the quantum states of one water molecule are involved in the hydration step (TS_2). The final step involves TS_3 and leads to a complex pattern of knitting and snipping.

Let us focus our attention on this transition structure. We present a more detailed picture in Figure 4. In Table I, the main components of the transition vector are displayed for the models with and without magnesium. The invariance shown by the common variables is remarkable. Actually, it is this invariance which grants the representation of the protein–substrate as a direct product. In Table II, the set of vibration frequencies is given for both models. Standard bond stretching frequencies are in the range of 2000 up to 4000 cm^{-1}. The vibration modes contain a bunch of low-frequency modes related to weakened bonds: those bonds that are to be knitted and those that are snipped once the electronic transition to the successor complex (product molded at the active site) is accomplished. It is appropriate to remember that one traditionally visualizes a picture of atom displacement amplitudes; our practical methods are extrapolations of semiclassical representations. But the picture, for chemical purposes, is good enough if we realize that a quantum dynamical process is taking place. The linear superposition of substrate and protein states, as described above, will evolve in time on the surface of the hypersphere. The system can relax onto a successor complex when the time evolution goes over a quantum state having nonzero amplitudes only on the quantum states of the products at the active site.

Discussion

The linear superposition principle has been used to consistently construct representations of molecular quantum states. All linear superposition states over bound MSs were mapped on a unit radius hypersphere. The time evolution involves swaths of trajectories on the surface of the hypersphere. Different moments of the mechanism are located on different regions of this surface. A full quantum dynamical description of the rubisco mechanism was constructed.

The formalism is based on the direct product space of the chemical system and the protein. Entangled states were not explicitly considered. The question now is do entangled states play a role in the mechanism? The answer is yes. One way to test

TABLE II
Vibration frequencies.

(a) 42 ($3N - 6$ with $N = 16$) vibration frequencies (cm^{-1}), ordered from 1 to 42, corresponding to the T-S for C—C and O—O bond breaking, 3C model

1	1756.34i	8	354.17	15	638.14	22	1149.59	29	1464.85	36	3136.08
2	103.12	9	366.16	16	661.87	23	1185.89	30	1527.39	37	3200.58
3	196.87	10	387.03	17	742.87	24	1315.51	31	1606.63	38	3277.22
4	202.48	11	426.29	18	895.68	25	1332.60	32	1625.21	39	3338.87
5	242.76	12	484.17	19	959.29	26	1365.41	33	1632.39	40	4119.52
6	269.82	13	545.17	20	1003.76	27	1398.72	34	1789.42	41	4159.52
7	332.92	14	616.58	21	1112.94	28	1439.24	35	2739.63	42	4182.91

(b) 87 ($3N - 6$ with $N = 31$) vibration frequencies (cm^{-1}), ordered from 1 to 87, corresponding to the T-S for C—C and O—O bond breaking model including the Mg coordination sphere

1	1659.47i	16	181.28	**31**	**459.82**	46	892.81	61	1485.07	76	2876.80
2	76.28i	17	188.30	32	500.12	47	923.02	62	1493.58	77	3065.90
3	64.00i	18	215.05	33	539.19	48	963.50	63	1500.05	78	3186.27
4	48.86i	19	231.66	34	560.96	49	1045.44	64	1548.14	79	3215.83
5	13.26i	**20**	**237.57**	35	573.67	50	1127.84	65	1557.58	80	3299.01
6	24.22	21	267.69	36	605.62	51	1147.29	66	1570.98	81	3361.05
7	56.26	22	279.06	37	609.75	52	1185.71	67	1574.52	82	3754.43
8	63.79	**23**	**304.56**	38	627.62	53	1230.91	68	1597.71	83	3783.48
9	77.59	**24**	**310.78**	39	687.52	54	1234.62	69	1615.77	84	3805.35
10	95.89	25	333.94	40	710.81	55	1247.48	70	1635.59	85	3942.22
11	108.43	26	352.24	41	740.17	56	1256.09	71	1774.36	86	4007.69
12	**133.60**	27	396.25	42	783.80	57	1349.19	72	1813.52	87	4137.35
13	**135.48**	28	400.42	43	832.98	58	1399.97	73	1835.83		
14	153.35	***29***	***424.83***	44	843.42	59	1465.61	74	1884.95		
15	**161.81**	***30***	***446.16***	45	859.01	60	1478.96	75	1915.22		

Bold figures refer to vibration frequencies with some amplitude on the Mg. Bold italics figures refer to vibration frequencies with significant amplitude on the Mg. The imaginary frequencies in the range 76i to 13i involve atoms in the magnesium coordination sphere. The important issue is that the imaginary frequency 1659i only has amplitudes for the reactant subsystem.

their importance was to recalculate all the transition structures with a model magnesium coordination sphere. For all of them, the carbon frame is basically invariant. This is good news for the consistency of the present partitioning approach. Is there any bad news? The answer is no. On the contrary, the enolization transition structure having the required electronic structure results from hydrogen bonding interactions with the carbamylated lysine residue. The catalytic activation appears to be dependent on the presence of this residue just as experimental workers had figured it out. In principle, such a result could not be obtained in the direct product basis even if we solved the exact time evolution equations. An intermolecular bond is typically an entangled state.

An important hypothesis was introduced to interpret the exact time evolution. For a given energy shell, the time evolution of the coherent states on the surface of the hypersphere would be an endless process. The arrival state is found away from the zone where the coherent state evolves. The unidirectionality of the reaction at the exit channel from TS_3, in line with previous discussions in a similar context, is evidence of the high density of states at this channel, in combination with efficient relaxation rates to other manifolds internal vibrational redistribution and electromagnetic fields). This is in the spirit of the "decoherence" interpretation in standard quantum mechanics [27]. Future experiments may shed light on verifiable differences between these two views.

Finally, we want to stress that the separability model used to study quantum mechanical time evolution is justified because the geometry and transition vectors in vacuum and in models incorporating portions of the active site are invariant. Of course, entanglements are important. But as discussed above, they can be included on a case-by-case basis.

EXORDIUM

The senior author (O.T.) would like to dedicate this article to the memory of Gilda Loew. I remember her, full of enthusiasm, in the early days of graphics assisted simulations of biomolecules. She led the way in applying computational methods to find original solutions for important problems in the biosciences. Her efforts to understand pharmacological and biochemical aspects from the standpoint of theoretical chemistry brought new substance into our quantum chemistry world. The present article tries to follow in the footsteps of Gilda Loew. It presents our attempts to understand enzyme catalysis. This time, a full quantum mechanics approach for time evolution is proposed. I do not know if she would have agreed with it. But I am sure that, she would have submitted the article to thorough discussion. Science makes progress by open confrontation of new ideas. She was an example of such openness.

ACKNOWLEDGMENTS

The Castellon group is indebted to the Servei d'Informàtica of the Universitat Jaume I for providing us with computer capabilities. M.O. thanks the Ministerio de Educación y Ciencia and Jaume I University for FPI fellowships. O.T. has been "Profesor Visitante IBERDROLA de Ciencia y Tecnología;" he thanks this organization for financing the visits to Spain, and NFR (Sweden) for continuing financial support over the years.

References

1. Oliva, M.; Safont, V. S.; Andrés, J.; Tapia, O. J Phys Chem A 2001, 105, 9243.
2. Oliva, M.; Safont, V. S.; Andrés, J.; Tapia, O. J Phys Chem A 2001, 105, 4726.
3. Safont, V. S.; Oliva, M.; Andrés, J.; Tapia, O. Chem Phys Lett 1997, 278, 291.
4. Oliva, M.; Safont, V. S.; Andrés, J.; Tapia, O. Chem Phys Lett 1998, 294, 187.
5. Andrés, J.; Oliva, M.; Safont, V. S.; Moliner, V.; Tapia, O. Theor Chem Acc 1999, 101, 234.
6. Schneider, G.; Lindqvist, Y.; Brändén, C.-I. Annu Rev Biophys Biomol Struct 1992, 21, 119.
7. Taylor, T. C.; Andersson, I. J Mol Biol 1997, 265, 432.
8. Cleland, W. W.; Andrews, T. J.; Gutteridge, S.; Hartman, F. C.; Lorimer, G. H. Chem Rev 1998, 98, 549.
9. Tapia, O. In Advanced Problems and Complex Systems; Quantum Systems in Chemistry and Physics, Vol. II; Hernandez-Laguna, A.; Maruani, J.; McWeeny, R.; Wilson, S., Eds.; Kluwer Academic Publishers: Dordrecht, 2000; p. 193.
10. Tapia, O. In Quantum Systems in Chemistry and Physics; Brändas, E. J.; Maruani, J.; McWeeny, R.; Smeyers, Y. G.; Wilson, S., Eds.; Academic Press, New York, 2001; Part 2.
11. Tapia, O. In New Trends in Quantum Systems in Chemistry and Physics; Maruani, J.; Wilson, S.; Smeyers, Y. G. Eds.; Kluwer Academic Publishers, Dordrecht, 2001; p. 23.
12. Tapia, O. J Mol Struct (Theochem) 2001, 537, 89.
13. Tapia, O. Adv Quantum Chem 2001, 40, 103.
14. Andersson, I. J Mol Biol 1996, 259, 160.
15. Yamaguchi, Y.; Osamura, Y.; Goddard, J. D.; Schaefer, H. E., III. A New Dimension to Quantum Chemistry: Analytic Derivative Methods in Ab Initio Molecular Electronic Structure Theory; Oxford University Press: New York, 1994.
16. Tapia, O.; Braña, P. J Mol Struct (Theochem) 2002, in press.
17. Dirac, P. A. M. The Principles of Quantum Mechanics; Clarendon Press: Oxford, 1947.
18. Sakurai, J. J. Modern Quantum Mechanics; Benjamin/Cummings: Menlo Park, CA, 1985.
19. Andrés, J.; Safont, V. S.; Tapia, O. Chem Phys Lett 1992, 198, 515.
20. Andrés, J.; Safont, V. S.; Queralt, J.; Tapia, O. J Phys Chem 1993, 97, 7888.
21. Tapia, O.; Moliner, V.; Andrés, J. Int J Quantum Chem 1996, 63, 373.
22. Dunbar, R. C.; McMahon, T. B. Science 1998, 279, 194.
23. Tapia, O.; Cárdenas, R.; Andrés, J.; Colonna-Cesari, F. J Am Chem Soc 1988, 110, 4046.
24. Tapia, O.; Oliva, M.; Safont, V. S.; Andrés, J. Chem Phys Lett 2000, 323, 29.
25. Van Dyk, D. E.; Schloss, J. Biochemistry 1986, 25, 5145.
26. Chène, P.; Day, A. G.; Fersht, A. R. J Mol Biol 1992, 225, 891.
27. Zurek, W. H. Phys Today 1991, 36.
28. Frisch, M. J.; Trucks, G. W.; Schlegel, H. B.; Gill, P. M. W.; Johnson, B. G.; Robb, M. A.; Cheeseman, J. R.; Keith, T.; Petersson, G. A.; Montgomery, J. A.; Raghavachari, K.; Al-Laham, M. A.; Zakrzewski, V. G.; Ortiz, J. V.; Foresman, J. B.; Cioslowski, J.; Stefanov, B. B.; Nanayakkara, A.; Challacombe, M.; Peng, C. Y.; Ayala, P. Y.; Chen, W.; Wong, M. W.; Andres, J. L.; Replogle, E. S.; Gomperts, R.; Martin, R. L.; Fox, D. J.; Binkley, J. S.; Defrees, D. J.; Baker, J.; Stewart, J. P.; Head-Gordon, M.; Gonzalez, C.; Pople, J. A. Gaussian 94; Gaussian, Inc.: Pittsburgh, PA, 1995.
29. Frisch, M. J.; Trucks, G. W.; Schlegel, H. B.; Scuceria, G. E.; Robb, M. A.; Cheeseman, J. R.; Zakrewski, V. G.; Montgomery, J. A., Jr.; Stratmann, R. E.; Burant, J. C.; Dapprich,

S.; Millam, J. M.; Daniels, A. D.; Kudin, K. N.; Strain, M. C.; Farkas, O.; Tomasi, J.; Barone, V.; Cossi, M.; Cammi, R.; Mennucci, B.; Pomelli, C.; Adamo, C.; Clifford, S.; Ochterski, J.; Petersson, G. A.; Ayala, P. Y.; Cui, Q.; Morokuma, K.; Malick, D. K.; Rabuck, A. D.; Raghavachari, K.; Foresman, J. B.; Cioslowski, J.; Ortiz, J. V.; Baboul, A. G.; Stefanov, B. B.; Liu, G.; Liashenko, A.; Piskorz, P.; Komaromi, I.; Gomperts, R.; Martin, R. L.; Fox, D. J.; Keith, T.; Al-Laham, M. A.; Peng, C. Y.; Nanayakkara, A.; Gonzalez, C.; Challacombe, M.; Gill, P. M. W.; Johnson, B.; Chen, W.; Wong, M. W.; Andres, J. L.; Gonzalez, C.; Head-Gordon, M.; Replogle, E. S.; Pople, J. A. Gaussian 98; Gaussian, Inc.: Pittsburgh, PA, 1998.

30. Gauss View 1.0; Gaussian, Inc.: Pittsburgh, PA, 1997.